Antiferromagnetism and *d*-wave superconductivity in cuprates: A cluster dynamical mean-field theory

A. I. Lichtenstein[1] and M. I. Katsnelson[2]
[1]*University of Nijmegen, 6525 ED Nijmegen, The Netherlands*
[2]*Institute of Metal Physics, 620219 Ekaterinburg, Russia*
(Received 22 November 1999)

We present an approach to investigate the interplay of antiferromagnetism and *d*-wave superconductivity in the two-dimensional Hubbard model within a numerically exact cluster dynamical mean-field approximation. Self-consistent solutions with two nonzero order parameters exist in a wide range of doping level and temperatures. A linearized equation for the energy spectrum near the Fermi level has been solved. The resulting *d*-wave gap has the correct magnitude and *k* dependence, but some distortion compared to the pure $d_{x^2-y^2}$ superconducting order parameter due to the presence of underlying antiferromagnetic ordering.

A microscopic theory of high-temperature superconducting cuprates (HTSC's) is still far from the final understanding.[1–3] One of the most important recent experimental achievements was the discovery of the pseudogap (PG) phenomenon above superconducting transition temperatures[4] and the existence of a sharp 41 meV resonance below T_c related with some collective antiferromagnetic excitations.[5] Recent neutron-scattering experiments[6] provide insight for the interesting problem on the origin of a condensation energy. Interplay of an antiferromagnetism (AFM) and *d*-wave superconductivity (*d*-SC) in cuprates could be a natural way of discussing different HTSC phenomena. This requires a quantitative electronic structure theory including two different types of the order parameters: AFM and *d*-SC. Within such an approach one can in principle analyze the phase diagram of HTSC compounds and resolve the long-standing problem of competition between antiferromagnetism and *d*-wave superconductivity in cuprates.[7,8]

A standard theoretical tool for cuprates electronic structure consists of the two-dimensional (2D) Hubbard model.[1] The importance of including the realistic tight-binding spectrum obtained from the local-density approximation (LDA) band structure analyses[9] was realized during the last years. Unfortunately, a most accurate quantum Monte-Carlo (QMC) simulation of a hole-doped 2D Hubbard model has difficulty in describing an interesting part of the HTSC phase diagram near 15% doping at the low temperature due to a so-called sign problem.[10] The perturbation theory of *d*-SC (Ref. 11) ignores the vertex corrections in the strong correlation case of HTSC. Great progress in the theory of the interacting fermions results from the developing of the dynamical mean-field theory.[12,13] While the antiferromagnetic phase is easy to incorporate in the single-site dynamical mean-field theory (DMFT) approach,[13] the *d*-wave superconductivity requires a cluster generalization of the DMFT. Different cluster-DMFT schemes have been proposed[13,14] and the recent application to the problem of the pseudogap in HTSC[15] has shown the efficiency of the cluster-DMFT approach. The investigation of a paramagnetic phase for the two-dimensional Hubbard model can be simplified using a translational symmetry,[14] while the problem of a coexistence of AFM and *d*-SC demands a broken-symmetry cluster calculation. It is equivalent to a multiorbital DMFT approach[16] and could be solved within the QMC method.[17]

In this paper we investigate the problem of antiferromagnetism and *d*-wave superconductivity in the two-dimensional Hubbard model using a cluster DMFT scheme.

The minimal cluster which allow us to study both AFM and *d*-SC order parameters on an equal footing consists of a 2×2 system in the effective DMFT medium (Fig. 1). We start with the extended-hopping Hubbard model on the square lattice:

$$H=\sum_{ij} t_{ij}c^{+}_{i\sigma}c_{j\sigma}+\sum_{i} U_i n_{i\uparrow}n_{i\downarrow},$$

where t_{ij} is an effective hopping and U_i local Coulomb interactions. We chose nearest-neighbor hopping $t=0.25$ eV and the next-nearest hopping $t'/t=-0.15$ for the model of $La_{2-x}Sr_xCuO_4$.[9] The total band width is $W=2$ eV and all Coulomb parameters set to be $U=1.2$ eV $(U/W=0.6)$. Let us introduce the ''supersite'' as a 2×2 square plaquet. The numeration of the atoms in the supersite is shown in Fig. 1. It is useful to introduce the superspinor $C^{+}_{i}=\{c^{+}_{i\alpha}\}$, where

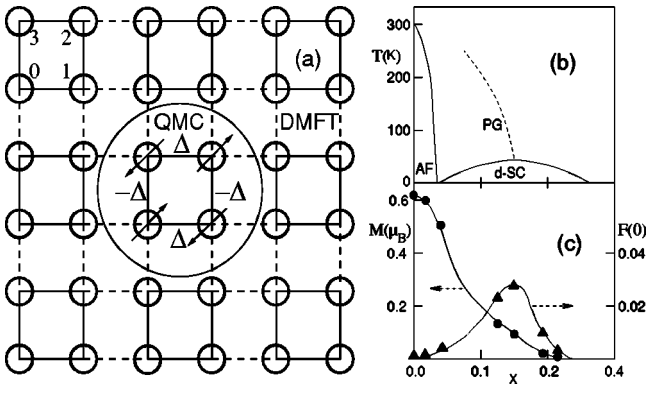

FIG. 1. (a) A schematic representation of an antiferromagnetic *d* wave 2×2 periodically repeated cluster; (b) a generic phase diagram of HTSC materials; (c) the calculated values of two order parameters: local magnetic moment *M* and *d*-SC equal time Green function $F^{01}(\tau=0)\equiv F(0)$ for different hole doping (*x*) at the inverse temperature $\beta=60$ eV^{-1} $(T=190$ K).

$\alpha=0,1,2,3$ (the spin indices are not shown). Taking into account the spin degrees of freedom, this is the eight-component superspinor creation operator. Then the crystal Green function for the Hubbard model can be rewritten as

$$G(\mathbf{k},i\omega)=[i\omega+\mu-h(\mathbf{k},i\omega)]^{-1},$$

where $h(\mathbf{k},i\omega)$ is the effective hopping supermatrix with the self-energy corrections and μ is the chemical potential. For simplicity we will write all the formulas in the nearest-neighbor approximations:

$$h(\mathbf{k},i\omega)=\begin{pmatrix} \Sigma_0 & t_x K_x^+ & 0 & t_y K_y^+ \\ t_x^* K_x^- & \Sigma_0 & t_y K_y^+ & 0 \\ 0 & t_y^* K_x^- & \Sigma_0 & t_x^* K_x^- \\ t_y^* K_y^- & 0 & t_x K_x^+ & \Sigma_0 \end{pmatrix}, \qquad (1)$$

where $K_{x(y)}^{\pm}=1+\exp(\pm ik_{x(y)}a)$, a is the lattice constant, and each element is 2×2 matrix in the spin space. Within the cluster-DMFT approach we introduce intra-atomic self-energy Σ_0 and interatomic self-energies Σ_x,Σ_y, and both functions are of the intrasite nature in the sense of our supersite:

$$\Sigma(i\omega)=\begin{pmatrix} \Sigma_0 & \Sigma_x & 0 & \Sigma_y \\ \Sigma_x^* & \Sigma_0 & \Sigma_y & 0 \\ 0 & \Sigma_y^* & \Sigma_0 & \Sigma_x^* \\ \Sigma_y^* & 0 & \Sigma_x & \Sigma_0 \end{pmatrix}.$$

The effective Hamiltonian defined through the translationally invariant ($\mathbf{k}$ dependent) self-energy corresponds to the renormalized energy dependent hoppings: $t_x=t+\Sigma_x, t_y=t+\Sigma_y$. The functions $\Sigma_0(i\omega),\Sigma_x(i\omega),\Sigma_y(i\omega)$ are found self-consistently within the cluster DMFT scheme[13] and for the d-wave superconduction state $\Sigma_x\neq\Sigma_y$. It is straightforward to generalize this scheme for a next-nearest-neighbor hopping as well as the long-range Green function and the self-energy. In this case we can renormalize also the second-nearest hopping: $t_{xy}=t'+\Sigma_{xy}$ for the 2×2 cluster, where Σ_{xy} (or Σ^{02}) is the nonlocal self-energy in the xy direction.

In the cluster version of the DMFT scheme,[13] or dynamical cluster approximation (DCA),[14] one can write the matrix equation for a so-called bath Green-function matrix $\mathcal{G}$ which describes an effective interaction with the rest of crystal:

$$\mathcal{G}^{-1}(i\omega)=G^{-1}(i\omega)+\Sigma(i\omega),$$

where the local cluster Green-function matrix is equal to $G_{\alpha\beta}(i\omega)=\Sigma_{\mathbf{k}}G_{\alpha\beta}(\mathbf{k},i\omega)$, and summation is run over the Brillouin zone of the square lattice. Note that in Eq. (1) we use translationally invariant self-energy obtained from the cluster DMFT similar to the DCA scheme.[14] The present ''matrix'' form of a cluster DMFT with the self-energy which is not periodic inside the cluster allows us to study a multicomponent ordered state.

In this case we have the standard DMFT problem with four ''orbital'' states per supersite. It is solved by the multiorbital QMC technique.[17] We use the generalized Nambu technique[18] to analyze the coexistence of the magnetic ordering and superconductivity. Let us introduce the superspinor

$$\Psi_i^+(\tau)\equiv(\psi_{1i}^+,\psi_{2i}^+,\psi_{3i}^+,\psi_{4i}^+)=(c_{i\uparrow}^+,c_{i\downarrow}^+,c_{i\uparrow},c_{i\downarrow})$$

and the anomalous averages describing the (collinear) antiferromagnetism $\langle c_{i\uparrow}^+ c_{j\downarrow}\rangle$ and the superconductivity $\Delta_{ij}=\langle c_{i\downarrow}c_{j\uparrow}\rangle$.

The generalization of the Hirsch-Fye QMC algorithm[19] for the superconducting problem[20] has been used. In the four-spinor case a discrete Hubbard-Stratonovich transformation has the following form:

$$\exp\left[-\Delta\tau U_i n_{i\uparrow}n_{i\downarrow}+\frac{\Delta\tau U_i}{2}(n_{i\uparrow}+n_{i\downarrow})\right]$$
$$=\frac{1}{2}\sum_{\sigma=\pm 1}\exp[\lambda_i\sigma(\psi_{1i}^+\psi_{1i}-\psi_{2i}^+\psi_{2i}$$
$$-\psi_{3i}^+\psi_{3i}+\psi_{4i}^+\psi_{4i})],$$

where $\lambda_i=\frac{1}{2}\operatorname{arccosh}[\exp(\frac{1}{2}\Delta\tau U_i)]$.

Since we take into account only the singlet pairing, there are the following nonzero elements of the d-SC energy gap parameters: $\Delta=\Delta_{01}=-\Delta_{12}=\Delta_{23}=-\Delta_{30}$. One can chose Δ_{ij} to be real and therefore symmetric: $\Delta_{ij}=\Delta_{ji}$. Separating normal and anomalous parts of the Green function we have

$$G(\mathbf{k},\tau,\tau')=\begin{pmatrix} G(\mathbf{k},\tau,\tau') & F(\mathbf{k},\tau,\tau') \\ F^+(\mathbf{k},\tau,\tau') & -G(-\mathbf{k},\tau',\tau) \end{pmatrix},$$

where $G(\mathbf{k},\tau,\tau')=-\langle T_\tau C_{\mathbf{k}}(\tau)C_{\mathbf{k}}^+(\tau')\rangle$, $F(\mathbf{k},\tau,\tau')=-\langle T_\tau C_{\mathbf{k}}(\tau)C_{-\mathbf{k}}(\tau')\rangle$ are the matrices in spin and ''orbital'' space. It is convenient to expand the anomalous Green function in Pauli matrices $F=(F^0+\mathbf{F}\sigma)i\sigma^y$ and use the symmetry properties:[21]

$$F^0(\mathbf{k},\tau,\tau')=F^0(-\mathbf{k},\tau',\tau)$$

$$\mathbf{F}(\mathbf{k},\tau,\tau')=-\mathbf{F}(-\mathbf{k},\tau',\tau).$$

Then a 4×4 spinor formalism is reduced to a 2×2 one in the collinear antiferromagnetic case with the d-wave superconductivity with the following spin-matrix form of the local Green function for the supersite:

$$G(\tau,\tau')=\begin{pmatrix} G_\uparrow(\tau,\tau') & F(\tau,\tau') \\ F(\tau,\tau') & -G_\downarrow(\tau',\tau) \end{pmatrix},$$

and the QMC formalism for the antiferromagnetic superconducting state is equivalent to the previous nonmagnetic one.[20] Using the discretization of the $[0,\beta]$ interval with L-time slices: $\Delta\tau=\beta/L$ ($\beta=1/T$ is an inverse temperature) the G_σ- and F- Green functions become the matrices of the $2NL$ dimension, where N is the number of atoms in the cluster. After Fourier transform to the Matsubara frequencies the Green-function matrix has the following form:

$$G(i\omega)=\begin{pmatrix} G_\uparrow(i\omega) & F(i\omega) \\ F(i\omega) & -G_\downarrow^*(i\omega) \end{pmatrix}.$$

In superconducting states the self-energy is defined as[13]

$$\mathcal{G}^{-1}(i\omega)-G^{-1}(i\omega)=\begin{pmatrix} \Sigma_\uparrow(i\omega) & S(i\omega) \\ S(i\omega) & -\Sigma_\downarrow^*(i\omega) \end{pmatrix},$$

and the inverse crystal Green-function matrix is equal to

$$G^{-1}(\mathbf{k},i\omega)=\begin{pmatrix} i\omega+\mu-h(\mathbf{k},i\omega) & s(\mathbf{k},i\omega) \\ s(\mathbf{k},i\omega) & i\omega-\mu+h^{*}(\mathbf{k},i\omega) \end{pmatrix},$$

where $s(\mathbf{k},i\omega)$ is the translationally invariant anomalous part of the self-energy $S(i\omega)$ similar to Eq. (1).

The two-component order-parameters state which includes the Neel antiferromagnetism and *d*-wave superconductivity [Fig. 1(a)] lowered the symmetry of the effective cluster-DMFT problem. A self-consistent DMFT cluster problem with AFM and *d*-SC general order parameters have been solved within the QMC scheme for the 8×8 matrix Green function with $L=64$ time slices. The resulting two order parameters for $\beta=60$ eV^{-1} ($T=190$ K) and $t'=0$ are presented in Fig. 1(c) together with the generic HTSC phase diagram [Fig. 1(b)] as a function of the hole doping. In this case the ordered magnetic moment is directly related with imaginary time Green function $G_{\sigma}(\tau)$: $M=G^{00}_{\uparrow}(0)-G^{00}_{\downarrow}(0)$, and for the *d*-SC order parameter we chose a positive value of superconducting imaginary time Green function $F^{01}(0)$. It is important that we find no serious sign problem for all QMC calculations with various doping levels, probably due to ''stabilized'' antiferromagnetic dynamical mean fields acting on the atoms in our 2×2 cluster. Note that the AFM cluster-DMFT solution exists for a much higher doping concentration than the experimental AFM ordered state and describes a dynamical mean-field version of AFM-spin fluctuations related to pseudogap phenomena [the PG region in Fig. 1(b)]. The maximum of the *d*-SC order parameter corresponds to the doping level of about 15% in agreement with the generic HTSC phase diagram. The *d*-SC order parameter is zero close to the undoped region ($x=0$), due to the presence of a large AFM gap. When the AFM gap is closed ($x\sim5\%$) the *d*-SC states develop, but for $x>20\%$, the *d* gap decreases again since the AFM spin fluctuations around the (π,π) point disappear.[2] The precise characteristic of the phase diagram including the interactions between the AFM and *d*-SC order parameters demands extensive cluster-DMFT calculations for the different temperatures and doping.

We would like to note that the existence of the *d*-SC cluster-DMFT solution for such high temperature does not necessarily mean that the superconducting transition temperature is larger than 190 K in our model. A crude estimation shows that the *d*-SC solution disappears at $T=300$ K for $x=0.15$ and the AFM solutions for $x=0$ become unstable at the temperature just above 1000 K. This could be the sign of a ''local'' AFM solution and a local *d*-wave solution, like local moments in magnetic systems.[22] Due to a multiscale nature of the problem under consideration—essentially different energies connected with local moment formation, long-range magnetic order, local *d*-wave pairs within the 2×2 plaquet, and finally coherent superconductivity—it is difficult to distinguish a real long-range ordering from slow dynamical fluctuations in our QMC simulations. We plan to separate these energy scales analytically and estimate superconductiong transition temperature in a future publication.

The role of next-nearest hopping is to lower the van Hove singularity[9] which increases the density of state at the Fermi level for the hole-doped case and favors the *d*-SC solution for a moderate correlation strength. There is also a change in the spin-fluctuation spectrum related with the broadening of the AFM peak near the (π,π) point due to the formation of so-called extended van Hove singularities with increase t'. We show one of the AFM *d*-SC solutions in Fig. 2 with the next-nearest-neighbor hopping for the 10% doping level and $\beta=50$ eV^{-1}. The resulting local magnetic moment is $M=0.28\mu_B$ and the *d*-SC order parameter $F(0)=0.036$. One can see that the superconduction order parameter is really of the $d_{x^2-y^2}$ symmetry since diagonal elements (F^{00}) as well as the next-nearest-neighbor elements (F^{02}) are all equal to zero, and only the nearest-neighbor superconducting Green functions (F^{01}) are nonzero and change the sign for F_x and

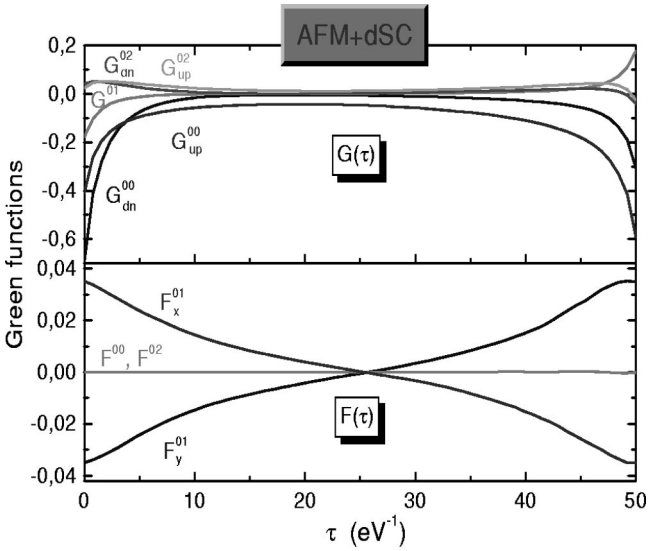

FIG. 2. The imaginary time normal (G_{σ}) and superconducting (F). Green functions for the 2×2 cluster-DMFT solution with second-nearest-neighbor hopping and inverse temperature $\beta=50$ eV^{-1} ($T=230$ K).

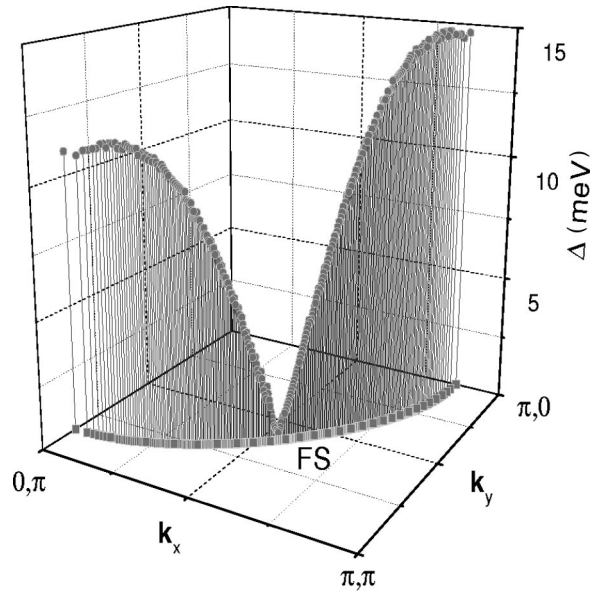

FIG. 3. The absolute value of the *d*-wave gap function at the Fermi surface for $x=0.15$, $t'=0$, and $\beta=50$ eV^{-1}.

F_y components. The normal local Green function (G^{00}) (plotted for the spin-up atom in Fig. 2) as well as (G^{02}) are spin split, while the nearest-neighbor Green function (G^{01}) has no spin splitting due to AFM spin symmetry (see Fig. 1). The absence of magnetic polarization in the nondiagonal G function along the $x(y)$ directions suppresses the magnetic pair breaking and makes the AFM d-SC coexistence possible.

In order to find the superconducting energy gap we solved a linearized equation for energy spectrum, assuming that the characteristic energy scale of $\Sigma_\sigma(i\omega)$ and $S(i\omega)$ are larger than the SC gap $\Delta(i\omega)$. In this case we can perform analytical energy continuations and the generalized equation for the energy spectrum has the simple form:

$$\det(H-EO)=0,$$

where $H=t(\mathbf{k})+\Sigma(0)-\mu$, $O=1-\Sigma'(0)$, and $\Sigma(0)=\int_0^\beta \Sigma(\tau)d\tau, \Sigma'(0)=\int_0^\beta \tau\Sigma(\tau)d\tau$. Note that $\Sigma(0)$ and $\Sigma'(0)$ in this expression should also be translationally invariant. We solve the linearized equation for energy spectrum (for $t'=0$ and $\beta=50$) and obtain the superconducting energy gap at the Fermi surface (Fig. 3). The topology of the Fermi surface was defined as the zero-energy contour for the energy spectrum with all the F Green functions set to be zero. It is clear that the symmetry of the d-wave state is not pure $d_{x^2-y^2}$ due to the underlying AFM states. This also means that the d-SC order could lower the symmetry of the AFM Neel state, and more general noncollinear magnetic states need to be investigated. Nevertheless the gap function has a maximum near the $(\pi,0)$ and $(0,\pi)$ points and is almost zero near the $(\pi/2,\pi/2)$ point. A magnitude of the maximum superconducting gap is of the order of 15 meV, in good agreement with experimental estimates,[4] and much smaller then the AFM gap for undoped case.

In conclusion, we present a nonperturbative analysis of the interplay between antiferromagnetism and d-wave superconductivity in the cluster dynamical mean-field theory for the Hubbard model. The maximum of the local magnetic moment corresponds to the half-filled case where the superconducting order parameter is vanished in contrast to the spin-fluctuation approach. We give a transparent physical explanation for a coexistence of the developed d-SC pairing with local AFM fluctuations at moderate doping.

We thank Gabi Kotliar, Antoine Georges, and Yurii Izyumov for helpful discussion.

[1] P. W. Anderson, Adv. Phys. **46**, 3 (1997).
[2] D. J. Scalapino, Phys. Rep. **251**, 1 (1994); J. Low Temp. Phys. **117**, 179 (1999).
[3] J. Schmalian, D. Pines, and B. Stojkovic, Phys. Rev. Lett. **80**, 3839 (1998).
[4] A. G. Loser, Science **273**, 325 (1996); H. Ding, Nature (London) **382**, 51 (1996); M. R. Norman *et al.*, *ibid.* **392**, 157 (1998); F. Ronning *et al.*, Science **282**, 2067 (1998).
[5] G. Aeppli *et al.*, Science **278**, 1432 (1997); M. A. Kastner *et al.*, Rev. Mod. Phys. **70**, 897 (1998); H. A. Mook *et al.*, Nature (London) **395**, 580 (1998).
[6] H. F. Fong *et al.*, Phys. Rev. B **61**, 14 773 (2000).
[7] E. Demler and S. C. Zhang, Nature (London) **396**, 733 (1998); W. Hanke *et al.*, Physica B **280**, 184 (2000).
[8] E. Dagotto, Rev. Mod. Phys. **66**, 763 (1994).
[9] O. K. Andersen *et al.*, J. Phys. Chem. Solids **56**, 1537 (1995).
[10] S. R. White *et al.*, Phys. Rev. B **40**, 506 (1989).
[11] N. E. Bickers, D. J. Scalapino, and S. R. White, Phys. Rev. Lett. **62**, 961 (1989).
[12] W. Metzner and D. Vollhardt, Phys. Rev. Lett. **62**, 324 (1989); A. Georges and G. Kotliar, Phys. Rev. B **45**, 6479 (1992); M. Jarrell, Phys. Rev. Lett. **69**, 168 (1992).
[13] A. Georges *et al.*, Rev. Mod. Phys. **68**, 13 (1996).
[14] M. H. Hettler *et al.*, Phys. Rev. B **58**, 7475 (1998).
[15] C. Huscroft *et al.*, cond-mat/9910226 (unpublished).
[16] A. I. Lichtenstein and M. I. Katsnelson, Phys. Rev. B **57**, 6884 (1998).
[17] M. J. Rozenberg, Phys. Rev. B **55**, R4855 (1997).
[18] L. N. Bulaevskii *et al.*, Adv. Phys. **34**, 175 (1985); Yu. A. Izyumov and V. M. Laptev, Int. J. Mod. Phys. B **4**, 447 (1990).
[19] J. E. Hirsch and R. M. Fye, Phys. Rev. Lett. **56**, 2521 (1986).
[20] A. Georges, G. Kotliar, and W. Krauth, Z. Phys. B **92**, 313 (1993).
[21] G. E. Volovik and L. P. Gor'kov, Zh. Éksp. Teor. Fiz. **88**, 1412 (1985) [Sov. Phys. JETP **61**, 843 (1985)].
[22] M. I. Katsnelson and A. I. Lichtenstein, J. Phys.: Condens. Matter **11**, 1037 (1999).